

Original Article

Experimental Investigation of Effect of Partial Replacement of Cement with Fly ash on the Workability and Mechanical Properties of Concrete

N. Z. Nkomo¹, A. A. Alugongo²

^{1,2}Department of Industrial Engineering and Operations Management & Mechanical Engineering, Vaal University of Technology, Vanderbijlpark, South Africa.

¹Corresponding Author : nkosilathin@vut.ac.za

Received: 20 May 2023

Revised: 28 June 2023

Accepted: 28 August 2023

Published: 03 September 2023

Abstract - Cement production contributes approximately 5% of the world's annual Carbon dioxide production. This high percentage can be attributed to the huge quantity of cement used worldwide. However, the process of production of cement is not environmentally friendly. Using fly ash as a partial cement substitute is a possible way to minimize pollution from cement production. Fly ash is produced as a by-product of burning coal in thermal power stations. The fly ash is mainly disposed of in landfills, contributing to environmental pollution, with only 20-40% of fly ash being used productively. This study investigates the effect of cement replacement with fly ash on concrete's workability and mechanical properties. The slump value increased with the incremental percentages of fly ash. The flexural strength increased with fly ash content, with the highest strength at 15%. The maximum compressive strength was observed at 15% fly ash content. The highest split tensile strength was observed at 20% fly ash content with a strength of 2.35 N/mm². The addition of fly ash into the concrete mixture ultimately had the effect of lowering the cost.

Keywords - Concrete, Fly ash, Mechanical properties, Workability.

1. Introduction

Fly ash, also known as Coal Combustion Residue (CCR), is a residue in the combustion of powdered, pulverized coal or lignite coal at high temperatures [1]. Fly ash is a residue of burning coal in thermal power stations. Fly ash is a complex heterogeneous material that consists of amorphous alumina silicate spheres, small quantities of iron-rich spheres, crystalline phases, and small quantities of unburned carbon [2]. Approximately 900 million tonnes of fly ash is generated worldwide, and a small percentage of approximately 30-40% is used productively [3]. In South Africa alone, 29 million tonnes of fly ash is produced per annum, with approximately 5% being used for value-added services [4]. The emission of fly ash particulates into the environment is controlled using scrubbers and mechanical and electronic precipitators in power stations. Fly ash makes up approximately 85% of the total coal residue and has a particulate diameter ranging from 0.5 to 100 µm [5].

The coal found and used in South Africa has been shown to have a high ash content. This phenomenon creates challenges in the use of the ash and its disposal. Fly ash that is used productively finds uses as additives or stabilizers in cement. The remaining percentage of fly ash is disposed of in landfills. Fly ash particles are generally spherical and have particle sizes less than 1 µm to 100 µm. Coal fly ash has many uses, such as cement additive in masonry blocks, a concrete admixture, lightweight alloys, and a concrete

aggregate. Fly ash enhances the performance of concrete in several ways. It reduces the requirement for mixing water and improves the paste flow behaviour [6]. However, innovative uses for fly ash are being researched, such as the fabrication of MMCs [7].

Fly ash obtained from various geographical locations lacks homogeneity. Thus, results obtained from various Class F fly ash can vary with its source, creating a problem in developing a universal model. This phenomenon necessitates the characterization of the raw materials at the target location to adequately predict the properties of the composite developed from this raw material. In this study, fly ash obtained from South Africa has been selected and studied.

Fly ash has been useful as a partial cement replacement in the construction industry [8, 9]. Several researchers have shown that incorporating fly ash can enhance the properties of concrete. However, further research is still necessary to determine the extent of variation in mechanical and workability properties with various mix ratios.

Fly ash, due to its pozzolanic activity, can be used as a cement replacement. Furthermore, using fly ash in this manner reduces the water quantity required in concrete paste, reduces bleeding and results in less heat evolution.



Kumer (2018) carried out research that recommended partial replacement of cement with fly ash at 15-25% for high-strength concrete. Fly ash allows dense concrete paste due to its spherically shaped particles, which allow dense packing of the fly ash particles [8]. In the last decade, about 6 million tons of greenhouse gas emissions have been avoided in the South African construction industry by using waste fly ash [9].

Furthermore, fly ash incorporation in concrete improves the strength properties [10], wear resistance [11], acid resistance and leaching properties [12].

This study aims to investigate the effect of adding fly ash on the concrete paste and the mechanical properties of concrete by varying the mix ratios according to the experimental design.

2. Materials and Methods

2.1. Physicochemical Characterization of Fly Ash

The fly ash was characterized prior to its use to ascertain its chemical composition and mechanical properties.

2.1.1. True Density

The fly ash sample was dispersed in water, and the amount of water dispersed per gram of fly ash gives the true density. The test was carried out according to ASTM C188 [13].

2.1.2. Moisture Regain

The moisture regained from the fly ash was measured by heating the fly ash to remove moisture using a hot air oven in accordance with ASTM D2974 [14]. The fly ash sample was then cooled and weighed. The weight reduction was reported as the moisture regain and recorded as a percentage. The moisture regain was calculated using equation 1.

$$\text{Moisture Regain (\%)} = \frac{\text{Initial weight} - \text{Oven dry weight}}{\text{Initial weight}} \times 100 \quad (1)$$

2.1.3. Morphology Analysis

The morphology of the fly ash particles was studied using an SEM with an EDS attachment. This analysis indicated the fly ash morphology, composition, and electrical conductivity. Before testing, the fly ash sample was coated with 5 nm gold using a Quorum Q150R ES Plus Machine. A JSM IT500LA JEOL SEM shown in Figure 1 was used to analyze the morphology of the fly ash particles through Back Scattered Electron imaging (BSE) and Energy Dispersive Spectroscopy (EDS).

2.1.4. Particle Size Distribution

The particle size distribution was determined by using laser light scattering using the Malvern 2000G instrument shown in Fig. 2 in accordance with ASTM D6941-19 [15]. The testing instrument measures particle sizes using the Fraunhofer and Mie theories, depending on the particle size.



Fig. 1 JEOL SEM Machine



Fig. 2 Malvern 2000G PSD analyzer

2.1.5. Determination of Active Phases

X-ray diffraction (XRD) analysis was used to analyze the active phases and structure of the fly ash particles. A Shimadzu XRD-7000 X-ray diffractometer machine, shown in Fig. 3 was used in accordance with ASTM C1365-18 standard. The source of radiation used in the XRD machine was Copper K α .



Fig. 3 XRD Diffraction analysis of fly ash sample on XRD-7000 shimadzu

2.2. Fresh Concrete Mixture

Concrete was mixed using the hand mixing method in accordance with SANS5861-1. The fly ash content was systematically varied between 15 – 30% with a water ratio of 0.6 for M20 concrete. The river sand used in the study had a fineness modulus of 3.69. Dolomite aggregates were used with a size of 13 mm and a flakiness index of 74.82%.

2.3. Workability of Concrete Mixture

Slump tests were done in accordance with SANS 5862-1:2006.

2.4. Testing of Specimens

Mechanical tests and non-destructive tests were carried out on the fabricated concrete slabs in accordance with ASTM and SANS standards.

2.4.1. Flexural Strength Test

The flexural strength of the concrete was determined using four-point loading in accordance with ASTM C78 (ASTM C78-00, 2004).

2.4.2. Compressive Strength Test

A compressive test was carried out in accordance with SANS 5836:2006 to determine the compressive strength.

2.4.3. Split Tensile Strength Test

The tensile test was carried out in accordance with ASTM C 596 -96 standard.

2.4.4. Rebound Hammer Test

A rebound hammer test was done in accordance with ASTM C806-02 (ASTM C806-02, 2004).

3. Results and Discussion

3.1. Fly Ash Physiochemical Characterization

The moisture regains, morphology, chemical composition and particle size distribution were investigated, and the results were discussed in the subsequent subsections.

3.1.1. Moisture Regain

The fly ash Moisture Regain (MR) was measured, and the results obtained are shown in Table 1. The average

moisture regain obtained from the test was 0.57%. This moisture regain is relatively low for Class F fly ash, which is normally approximately 2.71%, as reported in a study by Shreya et al. (2014).

The low moisture can be due to the thermal power station's high combustion temperature and efficiency. The fly ash was sourced from Lethabo Power Station, which has furnaces that reach high temperatures of 1200 °C at full load, giving high-efficiency combustion [16]. Combustion at elevated temperatures results in the breakdown of oxygen-containing groups, reducing the ash's MR.

The MR of fly ash has a direct bearing on the durability of the concrete. This phenomenon is due to water movement through concrete pores significantly compromising its durability due to the water eroding and weakening of the interfacial bonds within the concrete. A study by Pitroda et al. (2013) confirms this theory that water movement through concrete is a significant factor that can compromise its durability.

The permeability of concrete is related to the characteristics of its pore structure and the number of microcracks at the cement paste and aggregate interface.

Moreover, the pore structure involves the volume and size of the interconnected capillary pores, including fly ash particles. The pore structure provides transport of fluid into the concrete and subsequently affects its development and strength. However, other factors besides the constituent materials influence the water absorption of concrete, such as initial curing condition and duration.

Fly ash with a high moisture regain is not recommended for use in concrete. However, such fly ash may find use as a substitute for soil and gravel road embankments, as shown by a study carried out by Asokana et al. (2005).

The fly ash used in this study has an acceptable moisture regain of < 3 %, making it suitable for use in FRCC as it is considered acceptable by ASTM C618.

Table 1. Showing the moisture regain test on the fly ash sample

Time	1 Hour	2 Hours	4 Hours	24 Hours	28 Hours	30 Hours	
Test No.	W ₁	W ₂	W ₃	W ₄	W ₅	W ₆	% MR
1	5,0873	5,063	5,0632	5,0631	5,0643	5,0631	0,4757
2	4,0613	4,0299	4,0293	4,0288	4,0371	4,0288	0,8002
3	4,0115	3,9956	3,995	3,9935	3,9942	3,9935	0,4487
4	2,5568	2,5441	2,5443	2,5429	2,541	2,543	0,5397
5	6,6416	6,6414	6,6321	6,6219	6,6219	6,6219	0,2966
6	4,4226	4,4126	4,4101	4,4069	4,4076	4,4068	0,3573
7	3,2503	3,2416	3,2301	3,2197	3,2209	3,2209	0,9045
8	3,9263	3,9103	3,8997	3,8992	3,8975	3,8975	0,7335
Mean							0,57



Fig. 4 Dark grey fly ash sample

3.1.2. Colour

Figure 4 shows the dark grey colour of the fly ash used in the research. Fly ash colours vary from tan to dark grey. The colour of fly ash is a function of its chemical and mineral constituents. The dark grey colour observed indicates the high quantity of unburned carbon within the ash. This observation was confirmed with the EDS test, which recorded a greater than 20 % carbon content. Moreover, the colour of fly ash is also dependent on the iron content. The darker the shade, the higher the iron content. The fly ash used in this research was dark grey, implying a high amount of calcium oxides, and this was confirmed to be the case by the XRD and EDS results.

The fly ash used in this research is of intermediate lime content and may belong to either Class F or C, depending on the mineral constituents. However, tests done on EDS and XRD ascertained that the fly ash is Class F. PSD measured the particle size of the fly ash, and the results showed the fly ash of medium fineness consistent with the dark grey fly ash colour. The particle size and shape have a bearing on the colour of ash. Fine ash has a grey colour that gets increasingly darker as particle size and quantity of carbon increases. Furthermore, fly ash colour is also indicative of the lime content. However, not much research has been done on the dominant parameter that affects the fly ash's colour and the relationship between the mineral constituents and the particle size on the colour of fly ash.

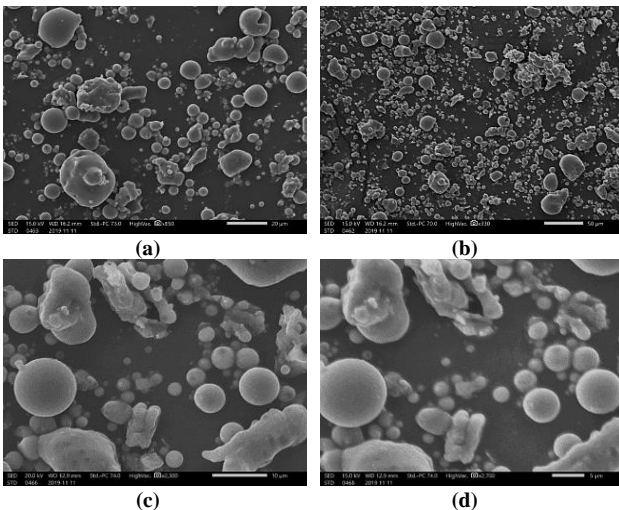


Fig. 5 Morphology of the fly ash particles

3.1.3. Surface Morphology of the Fly Ash

Figure 5 shows the morphology of the fly ash sample as observed under SEM.

The fly ash particles are seen to consist of vitreous spherically shaped particles with few irregularly shaped particles, as can be seen in Fig. 5a. Several elongated and angular-shaped particles exist between the spherical fly ash particles shown in Figure 5c.

These irregularly shaped particles are carbonaceous materials. The vesicular-shaped fly ash particles had limited exposure to the high temperatures during combustion; thus, their shape is like that of the pre-combustion particle form. The study by Kutchko & Kim (2006) and Sciubidlo et al. (2015) indicated that the shape of the fly ash particles is largely due to the combustion temperature and the cooling rate.

The larger size irregularly shaped particles can be due to silica ash and sulphate fume particles., as observed by Aaron Fuller et al. (2018). Regular-shaped fly ash particles give higher compressive strength due to fewer voids. When Figure 5 is critically examined, it is apparent that a high percentage of the particles are of a spherical shape. Therefore, the FRCC compressive strength is expected to be high.

Furthermore, due to the predominantly spherical-shaped particles, the fly ash is expected to give very good workability with concrete, as reported in a study by Saha (2018). The spherical shape of the fly ash particle improves the workability of concrete. The fly ash particles act like small ball bearings, making the concrete paste flow smoothly, making it easier to use and finish.

Furthermore, this reduces the amount of water required in the concrete mixture, as Jiang et al. (2000) reported. The particle morphology and size, as observed by Jiang et al. (2000), influence the concrete's water requirement and the strength development rate in hardened concrete. Finer and regular fly ash particles used in the present study would be expected to give concrete a higher rate of strength development.

This observation of fly ash morphology is consistent with research carried out by Rohilla et al. (2018). Rohilla et al. (2018) studied fly ash from Electrostatic Precipitator Heater (ESP) hoppers. They observed spherical-shaped particles and a few angular-shaped particles.

3.2. Particle Size Distribution

The fly ash Particle Size Distribution (PSD) is presented under the following two subheadings.

3.2.1. Particle Size Distribution using Particle Size Distribution Analyzer

Figure 6 shows the fly ash particle size distribution in this study.

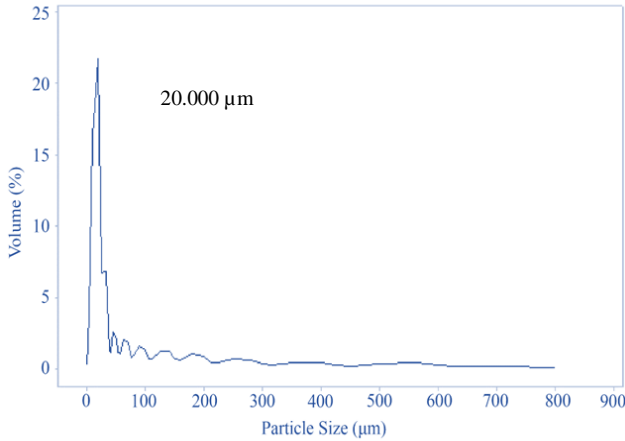


Fig. 6 Particle size distribution of fly ash

The fly ash particle sizes range from 0.31 µm to 800 µm. However, the largest volume of fly ash particles has specific sizes ranging from 5 µm to 32 µm. The highest quantity of fly ash of specific particle size is seen at 20 µm, with a volume of 21.75% falling within this particle size. After 32 µm, there is a sharp decline in the volume of particles with any specific size exceeding 32 µm.

The fly ash used in this study has over 50% of the particles having a particle size of < 20 µm, as shown in Fig. 6. This distribution implies that the ash has high pozzolanic activity; hence, these particles are suited for use in concrete to increase strength. In addition, the smaller particle size of fly ash generally indicates high-efficiency combustion and less amount of carbon content. This observation is supported by the SEM images, which show few large and irregularly shaped particles, implying high combustion efficiency.

Fly ash particle sizes < 10 µm are present in this fly ash sample and are expected to give better concrete compaction and reduce the water requirement in concrete. Furthermore, these particles were shown in a study by Masao et al. (1993) to strengthen the transition zone, give lower bleed quantity and increase the long-term compressive strength.

Fly ash particles > 45 µm are inferior compared to particles < 10 µm. These particles serve a major function of being fillers. Furthermore, there is a noticeable difference in tricalcium aluminate (C₃A) and mullite content, which tends to be higher in particles with < 10 µm than in particles > 40 µm. The higher content of these mineral elements imparts greater pozzolanic activity to the fly ash particles, giving concrete better mechanical properties. The highest volume of fly ash particle sizes is > 45 µm, indicating the presence of unburnt carbon. A large volume of unburnt carbon in fly

ash is unfavourable, as shown by a study carried out by Kearsley and Wainwright (2003). This phenomenon increases the water quantity required for a given concrete paste consistency.

The distance between two points equally spaced from the median is the span and governs the suitability of the fly ash for use in concrete. Table 2 gives the fly ash particle size distribution and span values. The formula for the span is as shown in Equation 1.

$$Span = d_{0.9} - d_{0.1} / d_{0.5} \tag{1}$$

The span value was 6.635 µm, which signified that the sample was homogeneous. The span value indicates the homogeneity or inhomogeneity of the ash. A small span value indicates that the sample is homogenous, whereas a high span value indicates that the sample is inhomogeneous.

However, the value of span obtained in this study is higher than that observed by Sarkar et al. (2012) from Indian power stations with a Span value of less than 3.13 µm. The difference between this current study and Sarkar et al. (2012) could be attributed to the higher combustion efficiency in the South African Lethabo power plant.

The average particle size is 17.610 µm and is indicated by d (0.5) size, as shown in Table 3. Furthermore, these results are consistent with research work by Mardon et al. [2008], Vassilev et al. [2005] and Dai et al. [2015] on similar-grade fly ash. Table 3 shows a comparison of Class F ash particle size distribution with research carried out in various geographic areas.

Fly ash consists of submicron size particles, which are respirable hence, pose a significant health risk as the particles are small enough to penetrate various organs in the human body. There is, therefore, a need for the fly ash to be handled with appropriate care, and suitable masks must be worn.

Table 2. PSD fly ash analysis results

Parameter	Value
Span	6.635 µm
Vol Weighted Mean D [4.3]	48.174
d (0.1)	3.183 µm
d (0.5)	17.610 µm
d (0.9)	120.029 µm

*D (0.1), D (0.5) and D (0.9) are percentiles from the particle size distribution curve

Table 3. Comparison of PSD distribution of fly ash

Particle Size Distribution	Present Study [South Africa]	Chandrapura [19] [India]	[20] [USA]	[21] [Spain]
d (0.1)	3.183 µm	2.02 µm	2.7 µm	2.8 µm
d (0.5)	17.610 µm	11.89 µm	15 µm	30 µm
d (0.9)	120.029 µm	117.70 µm	114 µm	98 µm

3.2.2. Particle Size Distribution using SEM

The fly ash particle size was obtained using direct measurement with the software on the SEM images, as shown in Fig. 7ure 7.

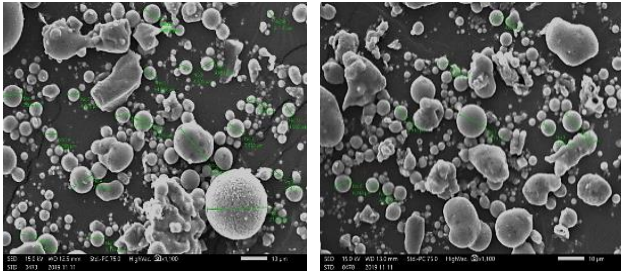


Fig. 7 Fly ash particle size measurement

Generally, the fly ash particle sizes ranged from 4 μm to 45 μm, as shown in Figure 7, which is consistent with the results obtained from the PSD analysis. Ramaswamy and Sharma's (2011) research observed that the finer the fly ash particles, the lower the water requirement for the concrete paste. Therefore, finer ash has a higher economy compared to coarse ash. These results imply that the fly ash would be suitable for partial cement replacement in concrete. Furthermore, using this type of fly ash could lower the cost of fabrication of the FRCC due to the lower water requirement in concrete paste formulation.

3.2.3. Chemical Composition Characterization

The chemical composition was characterized using EDS; the results are shown in Table 4.

Table 4. Data from energy dispersive X-ray spectrometer (EDS) elementary analysis of fly ash sample

Detection Spot	Elements (at %) as Detected by EDS								
	O	Al	Si	P	K	Ca	Ti	Mg	C
1	43.05	22.73	30.29	-	-	3.92	-	-	-
2	52.60	21.14	26.26	-	-	-	-	-	-
3	47.47	11.52	24.02	-	-	14.52	-	2.47	-
4	50.70	15.10	17.44	-	-	-	-	-	16.76
5	39.39	15.88	17.09	-	-	-	-	-	27.64
6	44.61	16.16	18.09	-	-	-	-	-	21.14
7	52.25	9.65	15.83	-	1.52	-	-	-	20.76
8	48.66	2.75	9.93	1.63	-	37.03	-	-	-
9	59.03	23.76	27.21	-	-	-	-	-	-
10	54.17	13.47	29.34	-	-	-	3.02	-	-
11	38.36	3.50	32.21	-	-	-	-	-	25.93
12	34.20	9.25	9.54	-	-	-	-	-	47.01

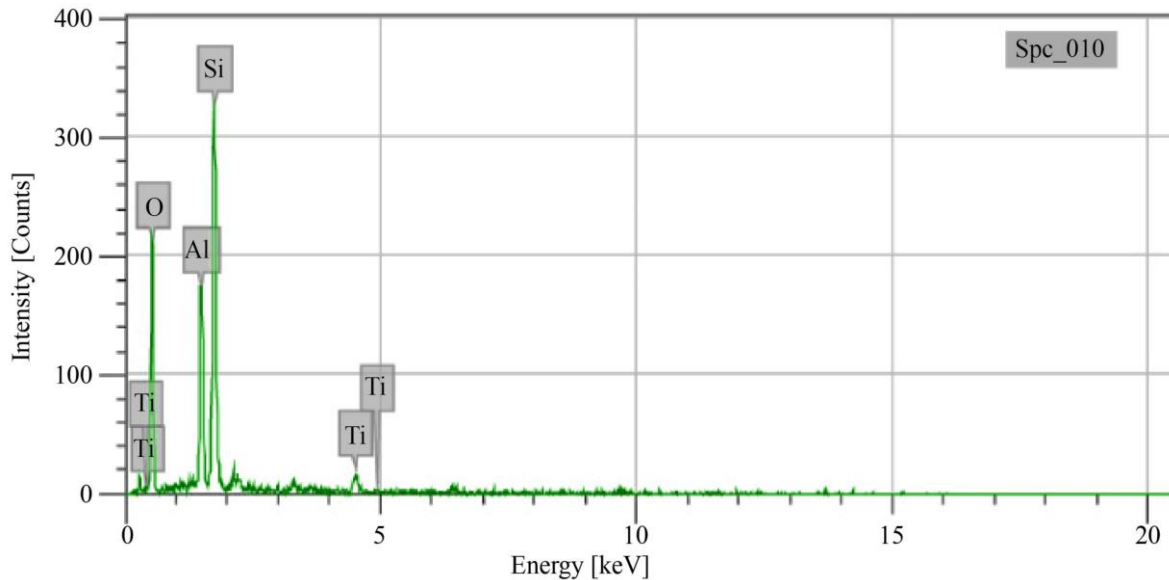


Fig. 8 Fly Ash EDS results

Table 4 shows the elements found within the fly ash sample as observed by EDS analyses. Different samples of fly ash were tested from the same batch. These were labelled the detection spots; the results from EDS analysis showed the

predominant elements in the fly ash samples to contain Calcium (Ca), Aluminium (Al), Phosphorus (P), Silicon (Si) and very small amounts of Titanium (Ti) and Magnesium (Mg).

These results indicated that the fly ash is Grade F due to the high silica and alumina content, which was observed to exceed 70%. The results showed homogeneity in the formulation of the fly ash sample with minor deviations due to the presence of trace elements such as Titanium. The EDS results are shown in Figure 8.

In general, the elements with a high concentration in the coal are also expected to have a high concentration in the fly ash as well. The results obtained here are consistent with the XRD results, which showed a high percentage of Calcium Aluminium oxide and Silicon oxide. The fly ash contains a small quantity of unburned carbon, which makes the ash suitable for use in concrete applications. Low carbon content in fly ash has a minimum effect on the air entrapment in concrete.

3.2.4. Chemical and Mineralogical Characterization

X-ray diffraction is a necessary analytical tool to identify and determine the constituent minerals in fly ash. The experimental results obtained from the XRD analysis are shown in Table 5.

The combined content of silicon, aluminium and iron oxides exceeded 70%. In accordance with ASTM C618, fly ash with the combined quantity of silicon, aluminium and iron oxides exceeding 70% is classified as Class F.

The XRD results show the presence of trace elements of heavy metals such as Magnesium (Mg), Titanium (Ti), and Iron (Fe), which could lead to ground pollution if the fly ash is not properly disposed of.

Figure 9 shows the XRD results for the fly ash sample. The high constituent of aluminosilicates of the ash contributes to its pozzolanic activity and makes it suitable for partial cement replacement in concrete.

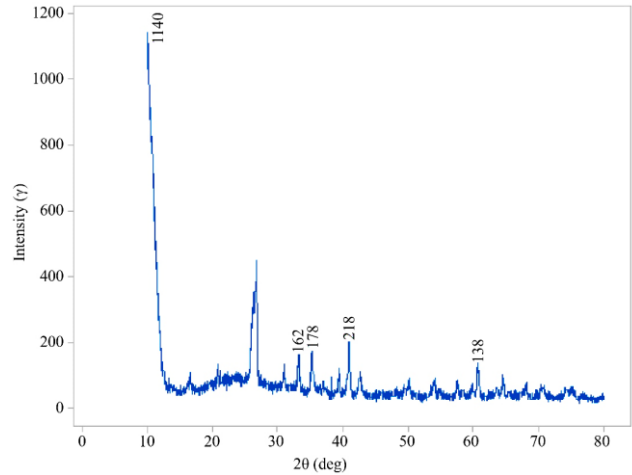


Fig. 9 XRD Pattern for fly ash particles

Table 5. XRD-based mineralogy of fly ash sample

Mineral	Formula	L	d	R
Potassium Graphite	C16K	0.545	0.610	0.333
Calcium Phosphide	CAP	0.571	0.579	0.331
Silicon Oxide (Tridymite-O)	SiO ₂	0.500	0.657	0.328
Calcium Aluminium Oxide	Ca12Al14O33	0.548	0.582	0.319
Sodium Sulfide	NaS ₂	0.472	0.668	0.315
Silicon Oxide	SiO ₂	0.490	0.618	0.311
Phosphorus	P	0.565	0.545	0.309
Aluminum Oxide	Al ₂ O ₃	0.556	0.552	0.308
Silicon Carbide (Moissanite-5H)	SiC	0.619	0.494	0.307
Magnesium Silicon	Mg ₂ Si	0.556	0.539	0.306
Sodium Calcium Phosphate (Buchwaldite)	NaCa(PO ₄)	0.529	0.565	0.300
Calcium Iron Oxide	CaFeO ₃	0.412	0.726	0.299
Iron Aluminum silicate (Almandine)	Fe2+2Al2(SiO4)3	0.563	0.519	0.299
Titanium Silicon	TiSi	0.565	0.517	0.292
Sodium Carbon	C32Na	0.500	0.574	0.287
Titanium Oxide	TiO ₂	0.600	0.478	0.287
Sodium Magnesium, Iron Titanium oxide silicon	Na ₃ (Mg3Fe+3Ti+4)Si8O22O2	0.455	0.628	0.286
Aluminium Titanium	Al ₂ Ti	0.500	0.569	0.285
Silicon Oxide (Tridymite-M. syn)	SiO ₂	0.411	0.685	0.281

The XRD pattern in Figure 9 shows many crystalline minerals like mullite (Al₆Si₂O₁₃) and quartz (SiO₂). These results are consistent with conclusions by Ayanda (2012) on ash from Matla Power station in South Africa. Cao et al. (2008) research stated that due to fly ash's high surface area,

condensation of trace elements tends to occur. The XRD pattern shows the presence of amorphous or non-crystalline content. The non-crystalline state can be seen by broad diffraction X-rays rather than sharp diffraction peaks. From Figure 9, the broad diffraction peaks represent the

amorphous structure observed from $25^{\circ} 2\theta$. The diffraction pattern shows that the major components include mullite, quartz and magnetite.

3.3. Effects of Fly Ash on Concrete Workability

Figure 10 shows the effect on slump value with an incremental percentage of fly ash replacement of cement.

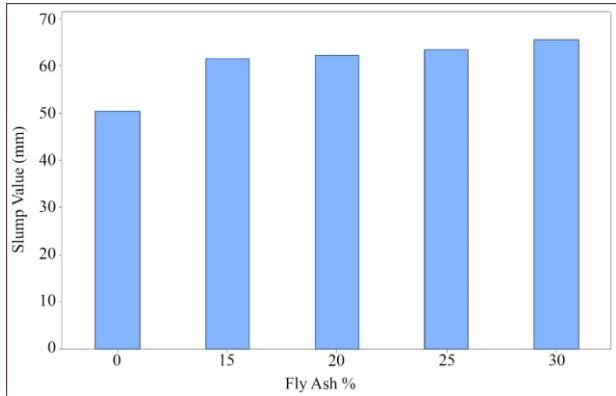


Fig. 10 Slump values of concrete paste with partial replacement with fly ash

Figure 10 shows that an increase in fly ash volume fraction increases the slump value. The slump increases significantly with the addition of 15% fly ash to 61.50 mm. After that, there was a marginal increase in slump value for each increment of fly ash. Figure 10 shows that the higher the fly ash content, the greater the workability of the concrete paste. The increase in slump value could be due to the flowability of the concrete paste containing fly ash. SEM showed the fly ash particle morphology to be predominantly spherical in shape and hence act as miniature ball bearings in the concrete paste, increasing its flowability. Concrete containing fly ash flowed better and consolidated better than conventional concrete.

Research by Shaikuthali et al. (2019) agreed with the trend observed in the current study. Shaikuthali et al. (2019) reported an increase in slump value from 155.00 mm for 10% fly ash replacement to 175.00 mm for 30% fly ash replacement. The high values observed by Shaikuthali et al. (2019) could be attributed to the slump measurement being observed and recorded after 120 minutes, unlike in the current study, where the slump value was taken within 5 minutes of removing the cone in accordance with SANS 5861-2. However, another Akmal et al. (2003) research showed an inverse trend. This could be attributed to the fact that the researcher used additives such as a superplasticizer in their research, which was not used in this study.

3.4. Effects of Fly Ash Addition on Concrete Compressive Strength

Figure 11 shows the effect of varying fly ash mass fractions on the compressive strength of 28-day concrete. The compressive strength of concrete increases sharply with cement replacement with fly ash up to 15%, as shown in Figure 11. The compressive strength improved significantly by adding 15% fly ash to 43 N/mm². After that, there is a slight decline with the addition of fly ash, as shown by 20%

fly ash replacement having a compressive strength of 41 N/mm². After that, adding 25% fly ash reduced the compressive strength drastically to 28 N/mm². After that, there is an increase in compressive strength with a further increase in fly ash, as shown by the strength of 30% fly ash replacement of cement, giving a strength of 36 N/mm². The compressive stress on the concrete followed a similar trend to the compressive strength, as shown in Figure 11.

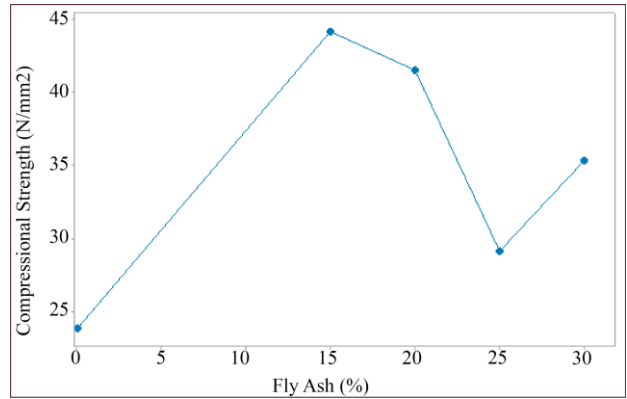


Fig. 11 Effects of fly ash addition on compressive strength

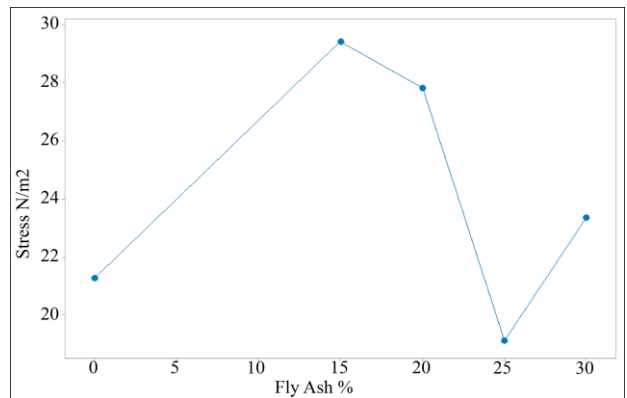


Fig. 12 Effects of fly ash addition on compressive stress of concrete

The maximum compressive stress was obtained at 15% fly ash addition, and after that, a decline in stress up to 25%. However, 30% fly ash added gave a moderate increase in compressive stress, as shown in Figure 12.

The results obtained in this research aligned with those obtained by Yerramala et al. (2012) and George et al. (2018), who both observed an initial increase in compressive strength with the addition of 15% fly ash. Research by Yerramala et al. (2012) recorded a significant drop in compressive strength of concrete containing 25% fly ash, and this result was consistent with the trend obtained in the present research. However, the research by Yerramala et al. (2012) focused on M10 concrete mix design; hence, the obtained compressive strength values were lower than those observed in the current study.

A study by Patel et al. (2012) reported a reduction in compressive strength with a fly ash volume fraction greater than 15%. Research by Chethan et al. (2015) and Sivakumar et al. (2015) observed a similar results trend to that obtained in this research, as shown in Figure 13.

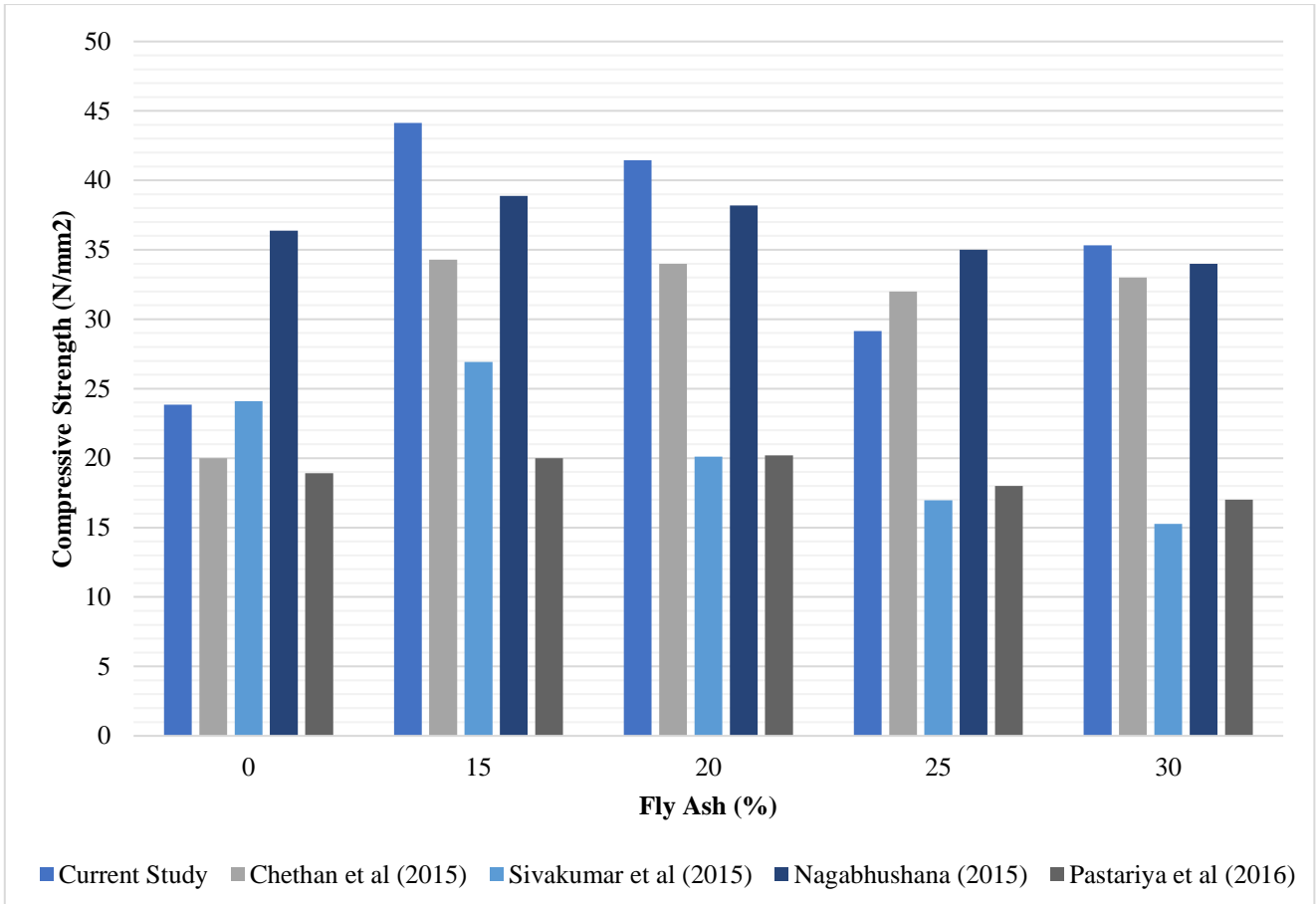


Fig. 13 Compressive strength comparison

From Figure 13 the highest compressive strength, as reported by Chethan et al. (2015), Sivakumar et al. (2015), Pastariya & Keswani (2016) and Nagabhushana (2015) was at 15% fly ash addition, which was in line with the results observed in this research.

However, the results obtained contrasted with a study by Joshi (2017), who reported a decline in compressive strength with the progressive addition of fly ash. The study reported a compressive strength of 19.64 N/mm² for 10% fly ash replacement and 18.07 N/mm² for 20% replacement. However, in the current study, the compression strength increased with an increase in fly ash replacement with 20% replacement, giving a compressive strength of 41 N/mm² higher than recorded in control. The divergent results can be attributed to the class of fly ash used.

3.5. Effects of Fly Ash Addition on Concrete Split Tensile Strength

Figure 14 shows the effect of fly ash addition on the split tensile strength of concrete.

The concrete's split tensile strength increased by adding 15% fly ash to 2.36 N/mm². After that, there was a marginal increase in split tensile strength with 20% fly ash content. After that, any further fly ash addition beyond 20% resulted in a decline in the split tensile strength. Further addition of fly ash to 30% reduced the split tensile strength further to 1.78 N/mm².

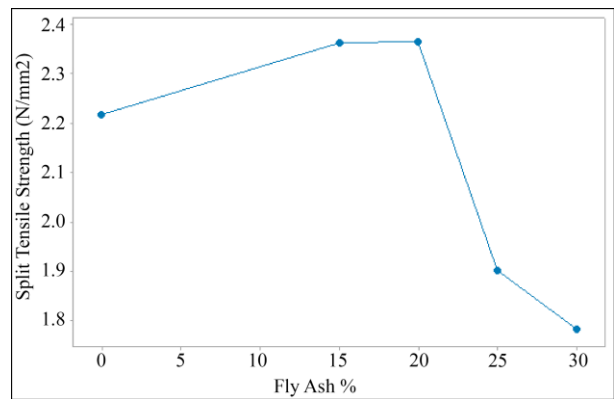


Fig. 14 Effect of fly ash on the split tensile strength of the concrete

The results obtained in Figure 14 are consistent with research by Yerramala et al. (2012). The initial increase in split tensile strength is due to increased the concrete paste's cohesiveness. According to research by Nagabhushana (2015), Nale et al. (2012) and Mullick (2005) the spherical shape of the fly ash particles improves the cohesiveness of the concrete mixture with minimum bleeding.

The use of fly ash in concrete can increase durability through a reduction in permeability, hence, its use in the construction of dams [22]. A comparison shown in Figure 15 with research by Sivakumar et al. (2015), Singh et al. (2017), and Nagabhushana (2015) showed a similar trend of results with the current research.

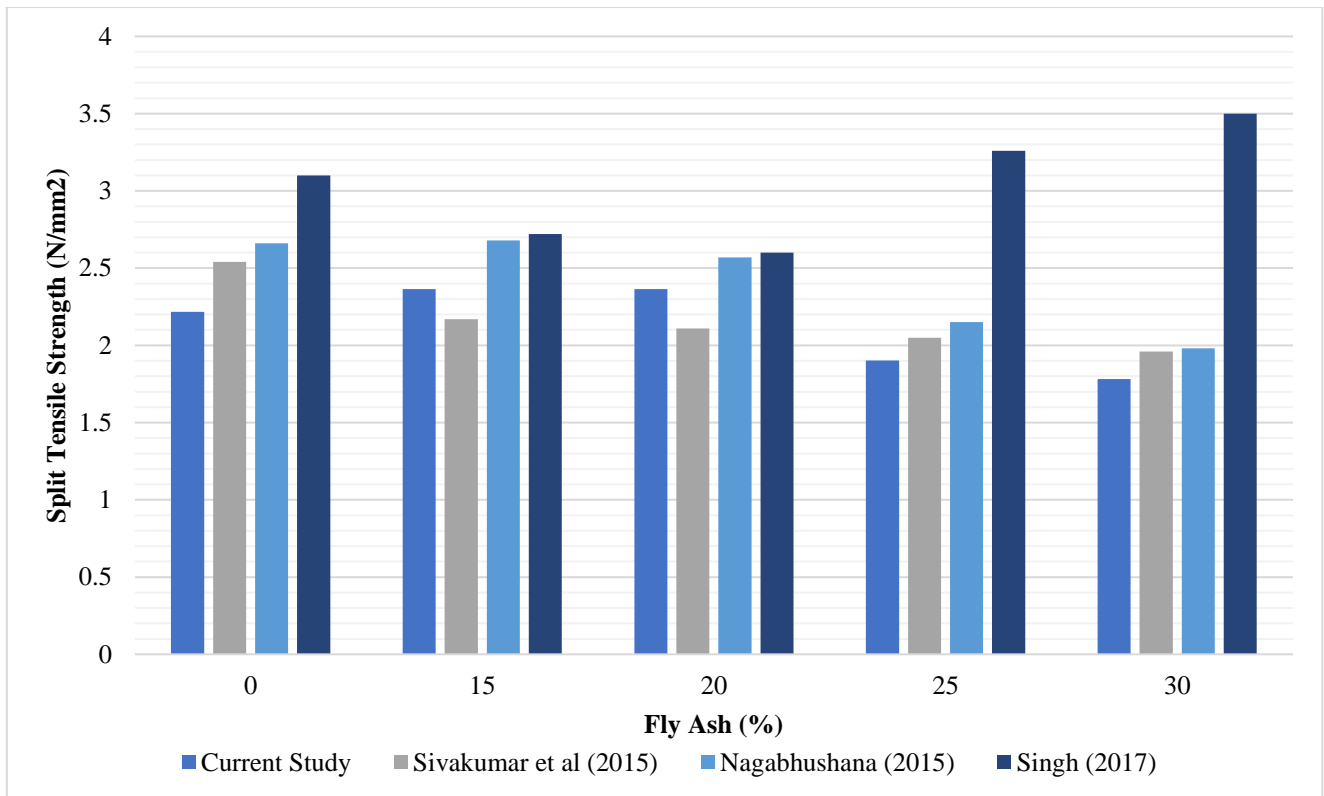


Fig. 15 Split tensile strength comparison

The comparative results in Fig. 15 show that the optimum fly ash addition is a 15% cement replacement. It can also be concluded that adding fly ash of > 25% has an adversative effect on the split tensile strength. Research by Singh et al. (2017) showed a significant increase in split tensile strength with 25% fly ash. This sharp increase could be attributed to the type of fly ash, which was bottom ash used by the researcher.

3.5. Effects of Fly Ash Addition on Concrete Flexural Strength

Figure 16 shows the effects of cement replacement with fly ash on the flexural strength of concrete.

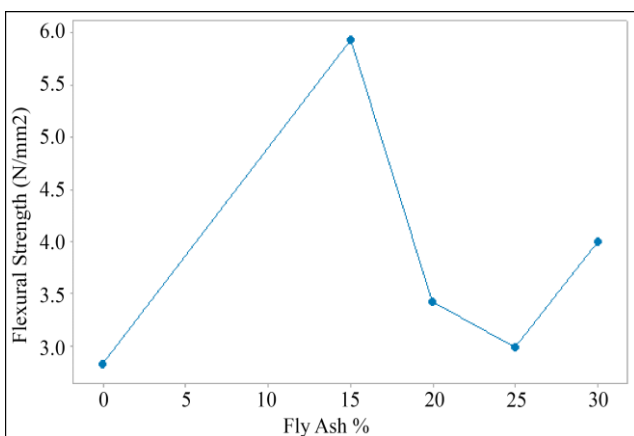


Fig. 16 Effect of fly ash on flexural strength

The addition of 15% fly ash has significantly improved the flexural strength of concrete. After that, any addition of fly ash reduced the flexural strength. There was a drastic

decrease in the flexural strength with 20% fly ash addition, giving a flexural strength of 3.42 N/mm². This decrease was still above the flexural strength of the control specimen.

Further, adding fly ash to 25% resulted in a further decrease in flexural strength to 2.99 N/mm². However, adding 30% fly ash increased the flexural strength marginally to 4.00 N/mm², greater than that of both 25% and 20% fly ash addition. The addition of 15% fly ash gave the highest flexural strength. The results obtained follow a similar trend to a study by Vinodsinh & Pitroda (2013) and Upadhyay et al. (2014).

The study by Nagabhushana (2015) and Upadhyay (2014) concluded a similar trend with an initial increase in flexural strength with a 15% volume fraction of fly ash, as shown in Figure 17.

Beyond 20% fly ash, an additional study by Nagabhushana (2015) and Upadhyay (2014) showed a marginal drop in flexural strength, contrasted with the present study. The reason for the low flexural strength observed in the current research could be due to poor packing and compaction of the concrete.

The study by Jayeshkumar et al. (2012) concluded that the progressive addition of fly ash reduced the flexural strength of the concrete. A study by Kazberuk and Lelusz (2007) highlighted that the strength gain of concrete containing fly ash is slower than that of concrete without fly ash. This implies that there is a possibility of a further increase in flexural strength beyond 28 days.

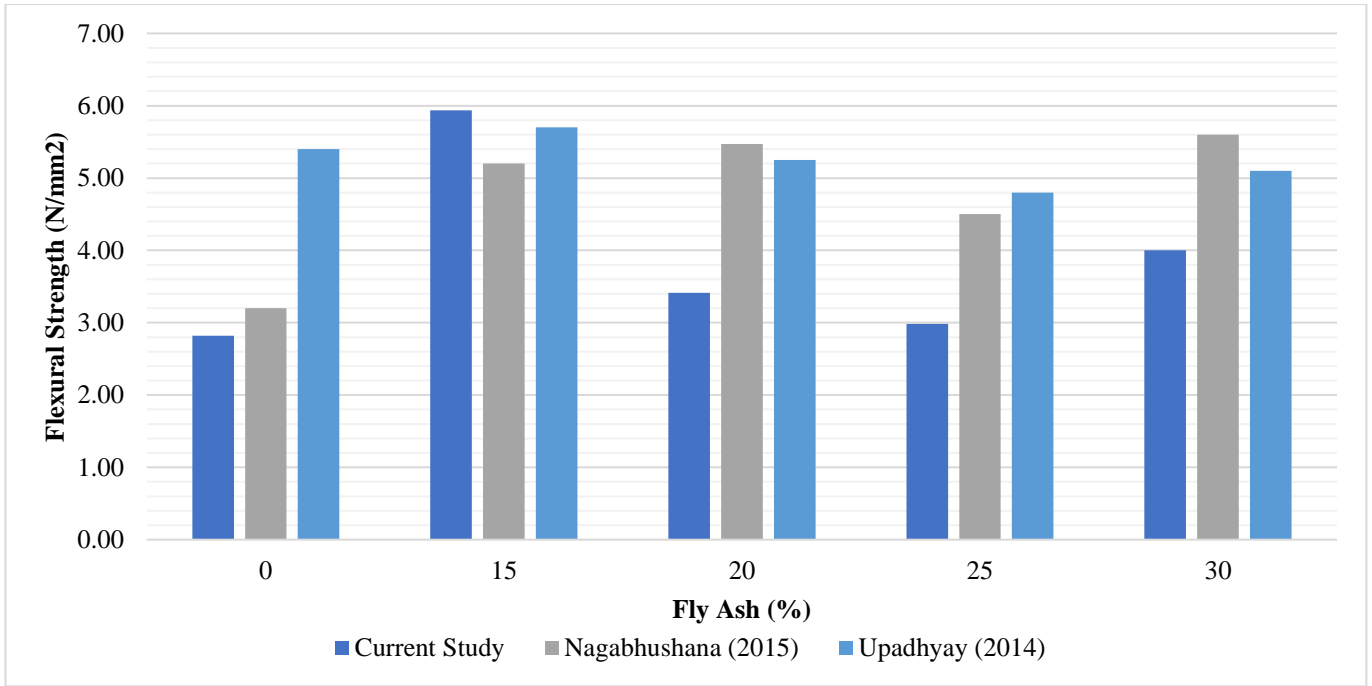


Fig. 17 Flexural strength comparison

3.5. Effects of Fly Ash on Rebound Number

Figure 18 shows the effects of fly ash on the rebound number.

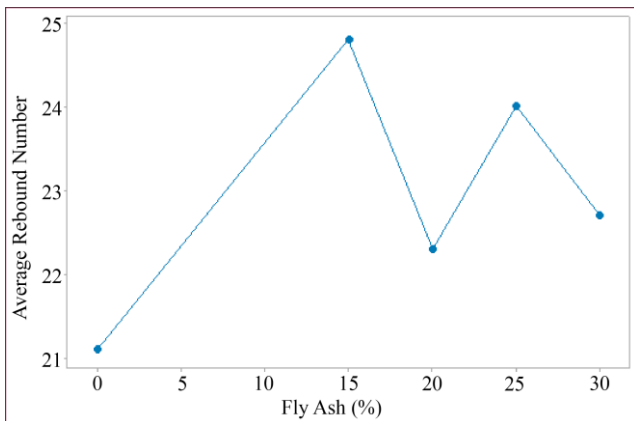


Fig. 18 Effect of fly ash addition on rebound number

The addition of 15% fly ash increases the rebound number to 24.8. After that, there was a decline in the rebound number with the addition of 20% fly ash to 22.3. Adding 25% fly ash resulted in a marginal increase in the rebound number to 24.0. Further, adding 30% of fly ash resulted in a drop in the rebound number to 22.7.

The rebound number obtained for all fly ash-containing samples in the study fell into the fair region of concrete quality based on the rebound number, as shown in Table 6. A comparison between the non-destructive rebound hammer compressive strength and the destructive cube test was made to establish a relationship between the two measurement techniques. This relationship was plotted on a graph, as shown in Figure 19. Table 6 shows a comparison between the current study and the rebound number obtained in a study by Reddy (2014).

Table 6. Comparison of rebound number

Fly Ash (%)	Current Study	Reddy V (2014)
0	21,10	20,00
15	24,80	21,00
20	22,30	20,00
25	24,00	18,00
30	22,70	17,00

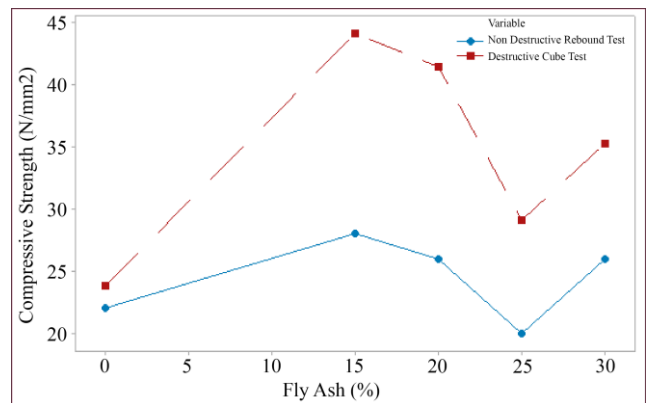


Fig. 19 Comparison between non-destructive and destructive cube test results

The trend obtained by Reddy (2014) agrees with the current study.

Figure 19 shows that the measurement of concrete compressive strength using the NDT rebound hammer method gives a significantly lower compressive value than the actual value obtained through compressive strength. The rebound hammer test is about 20–45% of the actual compressive strength, and this range is like a report given by Shaikuthali S (2019). The study reported that the NDT method gives 20-40% of the actual concrete compressive strength. From the results, it might seem there is no direct

correlation between the strength of the concrete and the rebound number. However, the similarity of the trend of the destructive and non-destructive tests in Figure 19 shows that within certain constraints, an empirical correlation exists between the compressive strength and the derived rebound hammer compressive strength. As shown in this study, this correlation requires calibration to suit the type of concrete being tested to give accurate results.

4. Conclusion

The conclusions that can be drawn from this research are as follows.

- The colour of fly ash observed in this study was dark grey colour, with a moisture regain of 0.5695%. The fly ash particles are mainly spherical in shape, as shown by the SEM. The fly ash particle size is between 0.31 μm and 800 μm .
- Chemical analysis indicated that the fly ash contained Ca, Al, P, Si, and small amounts of Ti and Mg. The XRD analysis indicated the presence of crystalline minerals such as mullite ($\text{Al}_6\text{Si}_2\text{O}_{13}$) and quartz (SiO_2).
- The river sand used had a fineness modulus of 3.69, which can be classified as coarse sand. The coarse aggregate used ranged from 9.5 to 13 mm.
- The slump value of the concrete paste was shown to increase with the incremental amounts of fly ash.

- The addition of 15 % fly ash increased the compressive strength. However, further addition beyond this percentage up to 30 % resulted in a reduction in compressive strength. However, fly ash addition at all percentages resulted in compressive strength above the control.
- Concrete containing incremental amounts of fly ash had increased split tensile strength. The highest split tensile strength was observed at 20% fly ash addition with a strength of 2.35 N/mm^2 .
- The addition of fly ash increased the flexural strength, with 15 % addition of fly ash giving a strength of 5.94 N/mm^2 , approximately double that of the control specimen. However, incremental amounts of fly ash beyond 15 % had a negative effect on the flexural strength.

Funding Statement

This study was funded by the Vaal University of Technology.

Acknowledgements

The authors wish to acknowledge the Department of Industrial Engineering & Operations Management and Mechanical Engineering at Vaal University of Technology for enabling this research.

References

- [1] Özer Sevim, and İlhami Demir, "Optimization of Fly Ash Particle Size Distribution for Cementitious Systems with High Compactness," *Construction and Building Materials*, vol. 195, pp. 104-114, 2019. [[CrossRef](#)] [[Google Scholar](#)] [[Publisher Link](#)]
- [2] Indrek Külaots, Robert H. Hurt, and Eric M. Suuberg, "Size Distribution of Unburned Carbon in Coal Fly Ash and its Implications," *Fuel*, vol. 83, pp. 223-230, 2004. [[CrossRef](#)] [[Google Scholar](#)] [[Publisher Link](#)]
- [3] N. Gamage et al., "Overview of Different Types of Fly Ash and their Use as a Building and Construction Material," *Digital Library University of Moratuwa, Sri Lanka*, 2011. [[Google Scholar](#)] [[Publisher Link](#)]
- [4] Jabulani S. Mahlaba, Elsabé P. Kearsley, and Richard A. Kruger, "Physical, Chemical and Mineralogical Characterisation of Hydraulically Disposed Fine Coal Ash from SASAL Synfuels," *Fuel*, vol. 90, no. 7, pp. 2491-2500, 2011. [[CrossRef](#)] [[Google Scholar](#)] [[Publisher Link](#)]
- [5] Radha Rani, and Manish Kumar Jain, "Physiochemical and Engineering Characteristics of Fly Ash and its Application in Various Field - A Review," *Journal of Biodiversity and Environmental Sciences*, vol. 6, no. 2, pp. 167-174, 2015. [[Google Scholar](#)] [[Publisher Link](#)]
- [6] Ankur Upadhyay, and Manish Kamal, "Characterization and Utilization of Fly Ash," Bachelor of Technology in Mining Engineering Thesis, National Institute of Technology, pp. 1-6, 2007. [[Google Scholar](#)] [[Publisher Link](#)]
- [7] Miloš Šešlija et al., "Laboratory Testing of Fly Ash," *Technicki Vjesnik*, vol. 23, no. 6, pp. 1839-1848, 2016. [[CrossRef](#)] [[Publisher Link](#)]
- [8] M. Ahmaruzzaman, "A Review on the Utilization of Fly Ash," *Progress in Energy and Combustion Science*, vol. 36, no. 3, pp. 327-363, 2010. [[CrossRef](#)] [[Google Scholar](#)] [[Publisher Link](#)]
- [9] S. Zulu and D. R. Allopi, "Optimising the Usage of Fly Ash in Concrete in the Construction of Roadworks," *Proceedings of the 34th Southern African Transport Conference*, 2015. [[Google Scholar](#)] [[Publisher Link](#)]
- [10] Watcharapong Wongkeo et al., "Compressive Strength and Chloride Resistance of Self-Compacting Concrete Containing High Level Fly Ash and Silica Fume," *Materials and Design*, vol. 64, pp. 261-269, 2014. [[CrossRef](#)] [[Google Scholar](#)] [[Publisher Link](#)]
- [11] Yingli Gao et al., "Effects of Nano-Particles on Improvement in Wear Resistance and Drying Shrinkage of Road Fly Ash Concrete," *Construction and Building Materials*, vol. 151, pp. 228-235, 2017. [[CrossRef](#)] [[Google Scholar](#)] [[Publisher Link](#)]
- [12] Ashish Kumer Saha, and Prabir Kumar Sarker, "Sustainable Use of Ferronickel Slag Fine Aggregate and Fly Ash in Structural Concrete: Mechanical Properties and Leaching Study," *Journal of Cleaner Production*, vol. 162, pp. 438-448, 2017. [[CrossRef](#)] [[Google Scholar](#)] [[Publisher Link](#)]
- [13] ASTM C188-17, Standard Test Method for Density of Hydraulic Cement, ASTM International, 2014. [Online]. Available: <https://www.astm.org/c0188-17.html>

- [14] ASTM, "ASTM D2974 Standard Test Methods for Moisture, Ash and Organic Matter of Peat and Other Organic Soils," *Americal Society for Testing and Materials*, 2000. [[Google Scholar](#)]
- [15] ASTM D6941-19 Standard Practice for Measuring Fluidization Segregation Tendencies of Powders, ASTM International, 2019. [Online]. Available: <https://www.astm.org/Standards/D6941.html>
- [16] ASTM C78/C78M-22, Standard Test Method for Flexural Strength of Concrete (Using Simple Beam with Third Point Loading), ASTM International, 2004. [Online]. Available: https://www.astm.org/c0078_c0078m-22.html
- [17] ASTM C805/C805M-18, Standard Test Method for Rebound Number of Hardened Concrete, ASTM International, 2004. [Online]. Available: https://www.astm.org/c0805_c0805m-18.html
- [18] Lethabo Power Station, Eskom, 2019. [Online]. Available: http://www.eskom.co.za/Whatweredoing/ElectricityGeneration/PowerStations/Pages/Lethabo_Power_Station.aspx
- [19] N. Shreya et al., "Fly Ash Characterization of Jharkhand (India) by Laser Granulometry and SEM/EDS," *Comunicacoes Geologicas*, vol. 101, pp. 851-854, 2014. [[Google Scholar](#)] [[Publisher Link](#)]
- [20] Jayanta Chakraborty, and Sulagno Banerjee, "Replacement of Cement by Fly Ash in Concrete," *SSRG International Journal of Civil Engineering*, vol. 3, no. 8, pp. 40-42, 2016. [[CrossRef](#)] [[Google Scholar](#)] [[Publisher Link](#)]
- [21] Dale P. Bentz, Andrew S. Hansen, and John M. Guynn, "Optimization of Cement and Fly Ash Particle Sizes to Produce Sustainable Concretes," *Cement and Concrete Composites*, vol. 33, no. 8, pp. 824-831, 2011. [[CrossRef](#)] [[Google Scholar](#)] [[Publisher Link](#)]
- [22] Joaquín Abellán-García et al., "Ultra-High-Performance Concrete with Local High Unburned Carbon Fly Ash," *DYNA SciELO*, vol. 88, no. 216, pp. 38-47, 2021. [[CrossRef](#)] [[Google Scholar](#)] [[Publisher Link](#)]
- [23] Priti A. Patel, Atul K. Desai, and Jatin A. Desai, "Evaluation of Engineering Properties for Polypropylene Fibre Reinforced Concrete," *International Journal of Advanced Engineering Technology*, vol. 3, no. 1, pp. 42-45, 2012. [[Google Scholar](#)] [[Publisher Link](#)]
- [24] Mohammed Abdul Samee et al., "Partial Replacement of Cement in Concrete with Fly Ash and Micro Silica," *SSRG International Journal of Civil Engineering*, vol. 4, no. 4, pp. 45-47, 2017. [[CrossRef](#)] [[Google Scholar](#)] [[Publisher Link](#)]
- [25] Diksha Chadha Vishnu Dev, Fly Ash Concrete, 2016. [Online]. Available: <https://www.slideshare.net/VishuPnhl/fly-ash-concrete-119055280>
- [26] Lokesh Rohilla et al., "An Experimental Investigation on the Effect of Particle Size into the Flowability of Fly Ash," *Powder Technology*, vol. 330, pp. 164-173, 2018. [[CrossRef](#)] [[Google Scholar](#)] [[Publisher Link](#)]
- [27] Khalid Saqer Alotaibi, and Khaled Galal, "Experimental Study of CFRP-Confined Reinforced Concrete Masonry Columns Tested Under Concentric and Eccentric Loading," *Composites Part B: Engineering*, vol. 155, pp. 257-271, 2018. [[CrossRef](#)] [[Google Scholar](#)] [[Publisher Link](#)]
- [28] Nhat-Duc Hoang, and Anh-Duc Pham, "Estimating Concrete Workability Based on Slumo Test with Least Squares Support Vector Regression," *Journal of Construction Engineering*, pp. 1-9, 2016. [[CrossRef](#)] [[Google Scholar](#)] [[Publisher Link](#)]